Energy Conversion and Management 113 (2016) 82–94

Contents lists available at ScienceDirect

Energy Conversion and Management

journal homepage: www.elsevier.com/locate/enconman

Development of heat pump and infrared-convective dryer and performance analysis for stale bread drying

Mustafa Aktaş [a,1], Seyfi Şevik [b,*], Burak Aktekeli [c]

[a] Energy Systems Engineering, Technology Faculty, Gazi University, Teknikokullar, 06500 Ankara, Turkey
[b] Electrical and Energy, Vocational School of Technical Sciences, Hitit University, 19169 Çorum, Turkey
[c] Worker Health and Safety, Osmaneli Vocational School, Bilecik Şeyh Edebali University, Osmaneli, 11500 Bilecik, Turkey

ARTICLE INFO

Article history:
Received 27 September 2015
Accepted 12 January 2016
Available online 5 February 2016

Keywords:
Heat pump dryer
Infrared dryer
Energy
Drying
Stale bread

ABSTRACT

This experimental study aims to develop a heat pump dryer (HPD) and an infrared dryer (IRD) also the comparative empirical analyses of these two methods and to analyze the drying kinetic of stale bread sliced 15 mm thickness and effectiveness on the drying kinetics of the stale bread of dryers. Dryers have been developed by using different techniques such as heat recovery unit, proportional control (PC) of drying air temperature, simultaneous control of the relative humidity–temperature–air flow rate, water cycle dehumidifier and closed-loop cycle to increase the drying efficiency of industrial drying applications. The highest coefficient of performance of the whole heat pump system ($COP_{ws,HP}$) was calculated as 3.7 and drying efficiencies of the IRD and HPD systems were calculated as 39% and 25%, respectively. When the HPD and IRD systems were compared in terms of drying time and energy consumption, it was observed that the IRD system did not only shortened the drying time up to 69%, but also decreased the energy consumption of the system by 43.2%. Based on the obtained results the effective moisture diffusivity (D_e) was calculated in the range from 8.3×10^{-8} to 3.2×10^{-7} m^2/s and mass transfer coefficient (h_m) was varied from 1.17×10^{-5} to 4.52×10^{-5} m/s. It was concluded that both dryers have significant effect in reduction of water content; the relative humidity controlled HPD can be applied efficiently for dryers and the dried stale bread can be reused as bread crumb by food industry.

© 2016 Elsevier Ltd. All rights reserved.

1. Introduction

Generation of heat or energy is the most prominent issue in drying processes. Heat pump dryers (HPDs) are significant components of the drying process due to their high performance. Utilization of HPDs can improve quality of dried products and reduce both drying time and energy consumption. However, there are still some limitations with the current HPD technology. Unfortunately, this technology cannot be operated with the system above the certain temperature level [1]. On the other hand, infrared dryer (IRD) exhibit significant advantages such as short drying time, operation capability at high temperatures, superior energy efficiency, better quality of ultimate dried product and less space requirement [2]. Sui et al. [3] stated that infrared drying had minimum damage on proanthocyanidins and polyphenols, best sterilizing effect and shorter drying time. Jaturonglumlert and Kiatsiriroat [4] reported that the combined convective and far-infrared drying process exhibited shorter drying time due to the higher heat and mass transfer coefficients compared to the hot air drying. Also, Nowak and Lewicki [2] revealed that drying time can be reduced to 50% in the infrared drying process comparing with infrared drying process with a convective drying process having equivalent empirical parameters.

Heat pump [1,5–8] and infrared [2,3,9] technologies have important advantages for drying systems. These systems can be used both combined and alone. There are numbers of studies investigating combined/single drying processes in the literature, such as HPD [10–12], photovoltaic-solar HPD for different food products [1], heat pump-microwave dryer for green peas [13], gas engine heat pump (GEHP) for food drying processes [14], IRD for red pepper [15], hot air-IRD [16–17], IR-HPD for squid fillets [18], IR assisted microwave dryer for bread crumbs [19], which have resulted in reduction of drying time and saving in energy consumption compared to the conventional drying methods.

In the present study, stale bread processing was preferred to conduct IRD and HPD tests. In the experiments, dried stale bread is white type. Content of white type bread was given in Table 1

* Corresponding author. Tel.: +90 364 223 08 00.
E-mail addresses: mustafaaktas@gazi.edu.tr (M. Aktaş), seyfisvk@hotmail.com (S. Şevik), burak.aktekeli@bilecik.edu.tr (B. Aktekeli).
[1] Tel.: +90 312 202 87 07.

http://dx.doi.org/10.1016/j.enconman.2016.01.028
0196-8904/© 2016 Elsevier Ltd. All rights reserved.

Nomenclature

A_s	product surface area, m^2
c	specific heat capacity, kJ/kg K
D_e	effective diffusivity coefficient, m^2/s
EU_{ter}	thermal energy consumption, kJ
EU_{mec}	mechanical energy consumption, kJ
h	enthalpy, kJ/kg
h_{fg}	latent heat, kJ/kg
h_m	mass transfer coefficient, m/s
$\hbar$	convection heat transfer coefficient, W/m^2 K
L	product thickness, m
Ls	tray length, m
k	thermal conductivity of air, W/mK
M_i	initial wet weight, g
M_d	final dry weight, g
M_t	moisture content at time "t", g water/g dry matter
M_{t+dt}	moisture content at time "t+dt", g water/g dry matter
M_e	equilibrium moisture content, g water/g dry matter
M_0	initial moisture content, g water/g dry matter
m	mass, kg
$\dot{m}$	mass flow rate, kg/s
n	revolution per minute, rpm
$\dot{Q}$	heat flux, kW
Q_m	energy for product heating, kJ
Q_w	energy for moisture evaporation, kJ
P	power, kW
R	function uncertainty
T	temperature, °C
t	drying time, h
u	velocity, m/s
$\dot{V}$	volumetric flow rate, m^3/s
υ	kinematic viscosity, m^2/s
$\dot{W}_{Comp}$	compressor power, kW
$\dot{W}_F$	fan power, kW
$\dot{W}_P$	pump power, kW
W_R	total uncertainty, %
w_1, w_2, w_n	independent variables uncertainties
x	independent variables
ΔP	pressure difference, mbar
η	efficiency

Abbreviations

COP	coefficient of performance
DAVM	drying air velocity measurement
DAV	drying air velocity
DAT	drying air temperature
DR	drying rate, g water/g dry matter per minute
HA	hot air
HAIRD	hot air infrared dryer
MC	moisture content, g water/g dry matter
SEC	specific energy consumption, kJ/kg
SMER	specific moisture extraction rate, g/kW h
TEC	total energy consumption, kW h

Subscripts

C	condenser
ec	energy consumption
ee	energy efficiency
eq	equilibrium
eV	evaporation
de	drying efficiency
i	inlet
ia	inlet air
o	outlet
oa	outlet air
p	product
re	recovery
s	surface
w	water
ws	whole system

[20]. Bread goes stale in a short time during its storage at the ambient temperature. Thus, relative bread wasting is in significant amounts in the world. For example, according to the research conducted in Turkey in 2012, 2.1 billion loaves of bread are wasted annually [21]. Accordingly, bread manufacturers use different food additives to increase their shelf-life and/or recycle stale breads through drying techniques. Available literature studies on the drying characteristics of stale bread are limited. John et al. [22] investigated drying processes of bread and biscuit crumbs by means of a fluidized-bed dryer based on the particle size distribution, fluidization behavior and the relevant drying kinetics. Basman and Yalcin [23] concerned with the quality change in noodle during the infrared drying process. They observed that infrared drying increased the rate of the moisture loss. Tireki et al. [19] dried the bread crumb dough using conventional, infrared, microwave and infrared-assisted microwave dryer. In their study, based on conventional dryer, the drying time decreased 80.2–94.0% in IRD.

The present empirical study aims to increase drying efficiency through developing the HPD and IRD systems at low drying air temperature (DAT). Thus, individual HPD and IRD systems were designed and developed by using different techniques of DAT-relative humidity (RH)-drying air velocity (DAV) control, proportional control (PC) of infrared power; and using a heat recovery (HR) unit. Then, these dryers were compared to analyze the drying efficiencies. Another aim was to investigate the behavior of the stale bread during drying process. On the other hand, this study has a social aim by focusing on issue of bread wasted preventing in daily consumption. Structure of this study was exhibited in Fig. 1.

2. Materials and methods

2.1. Experimental setups

In this study, dryers (IRD and HPD) were designed, manufactured and developed. Re-utilization of waste heat of drying air has been aimed to increase the drying efficiency of HPD and IRD.

2.1.1. HP dryer

A closed-loop HPD was designed and manufactured to obtain high level of performance coefficient (COP) and drying efficiency (Fig. 2). In dryer, simultaneous control of the relative humidity (RH), temperature (T) and air flow rate without auxiliary heat source can be accomplished. Condensation and evaporation temperatures of heat pump system have been determined based on the desired Psychrometric conditions of drying air and thermodynamic balance of drying system. Heat balance of the system was ensured by the cold water tank. Stored cold water obtained in the cycle was used to dehumidification of drying air during the drying processes. As the physical properties of air were suitable, either fresh air from outside can be taken in or waste air can be exhausted by variable air volume (VAV) boxes. VAV boxes can be

Table 1
Content of white-type bread [20].

White bread	Moisture (g)	Protein (g)	Energy (Cal)	Carbohydrate (g)	Calcium (mg)	Iron (mg)	Vitamin B_1 (mg)	Vitamin B_2 (mg)	Niacin (mg)
(100 g)	31.8	9.1	276	56.6	7	0.7	0.09	0.06	0.8

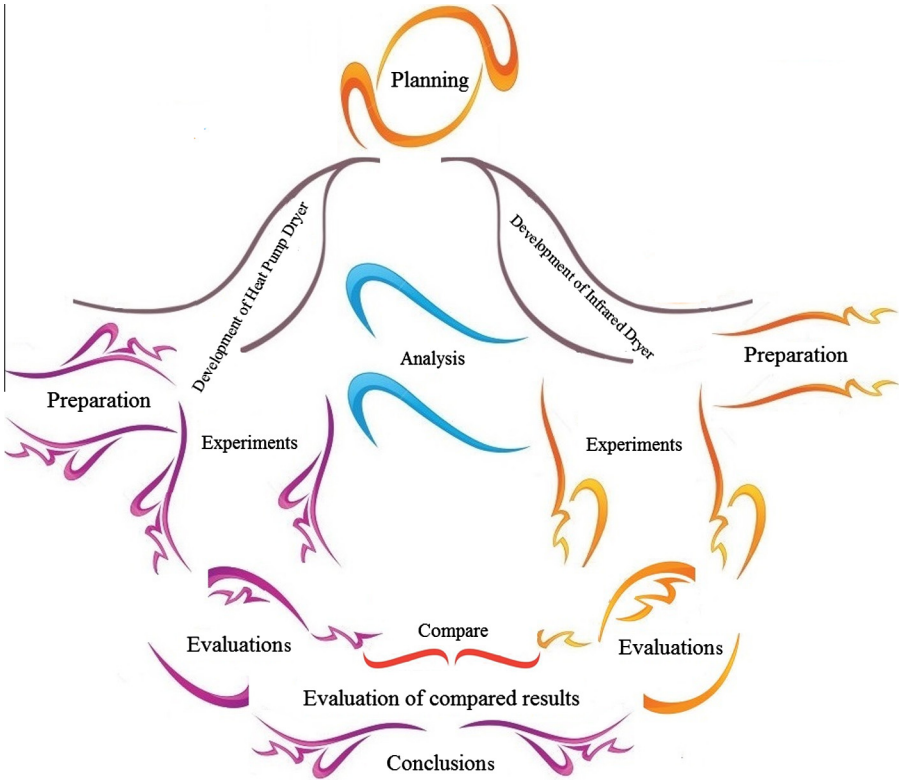

Fig. 1. Structure of study.

used in appropriate weather conditions in terms of relative humidity and temperature values of air. The equipments used in the HPD with its technical characteristics were shown in Table 2. The HPD was equipped by measurement instruments, sensors and a recording device, which made it possible to control air conditions. Technical properties, accuracies, uncertainties and measurement equipment were shown in Table 3.

Components of the system are controlled through a programmable logic controller (PLC) system. Also, a control algorithm is developed to manipulate the HPD easily and efficiently. Accordingly, while all controllable drying parameters determined during the pre-analysis of the dryer can be entered from the PLC screen, measured values (temperature, relative humidity, product mass, and air velocity) can be monitored and recorded on computer during the experiments. The air flow and the PLC system diagram of the HPD system are shown in Fig. 3. Where TRH_3 is the temperature and relative humidity of drying air measured at the inflow of the drying cabinet, TRH_1 is the temperature and relative humidity of drying air measured at the outflow of the drying cabinet, TRH_2 is the temperature and relative humidity of drying air after cooling serpentine; the DAVM is drying air velocity measurement and the PMM is product mass measurement. The control system of the HPD is shown in Fig. 4. In the HPD, the DAT and the RH are controlled according to the set values. Desired air flow rate is provided by a fan with frequency converter. DAV is controlled through the Proportional–Integral–Derivation (PID) control. The DAV is controlled by frequency control in line with the desired value. Thus, the HPD can be operated successfully through the PLC system in order to maintain desired drying air conditions.

2.1.2. IR dryer

IRD system was designed by considering the energy efficiency with-or-without HR. The IRD system consists of near infrared (NIR) lamps, a controller, sensors, load cell unit, drying cabinet and a HR unit (Fig. 5). Technical properties and accuracies of measurement equipment, uncertainties and sensors are shown in Table 3. The equipment used in the IRD and their technical characteristics are shown in Table 4.

Dryer was equipped with a load cell to observe dried product mass during the drying process. Temperature of dried material is measured by means of a K-type thermocouple. The temperature sensor is contacted with surfaces of product on the side that is not exposed directly to infrared radiation. According to this way, misleading measurements is eliminated. Six rod types NIR lamps (6×500 W) were mounted in three rows; they were assembled in the dryer cabinet, each of them was emitting radiation with a peak wavelength of 2400 nm.

An electronic control board was developed to adjust both the DAT and the DAV values in IRD. In order to obtain desired drying air temperature, the DAT is controlled proportionally by adjusting the power of infrared lamps. Thus, the temperature fluctuation that may occur in the infrared drying system is prevented through PC. DAT is kept within ±0.3 °C offset in the drying cabinet. A linear relationship is established between the controlled variable and controlled device and an energy balance is set via heat and mass transfer equations between the required energy and the dried product. The drying kinetics of the product is highly depended on the distance between the infrared heaters and the product.

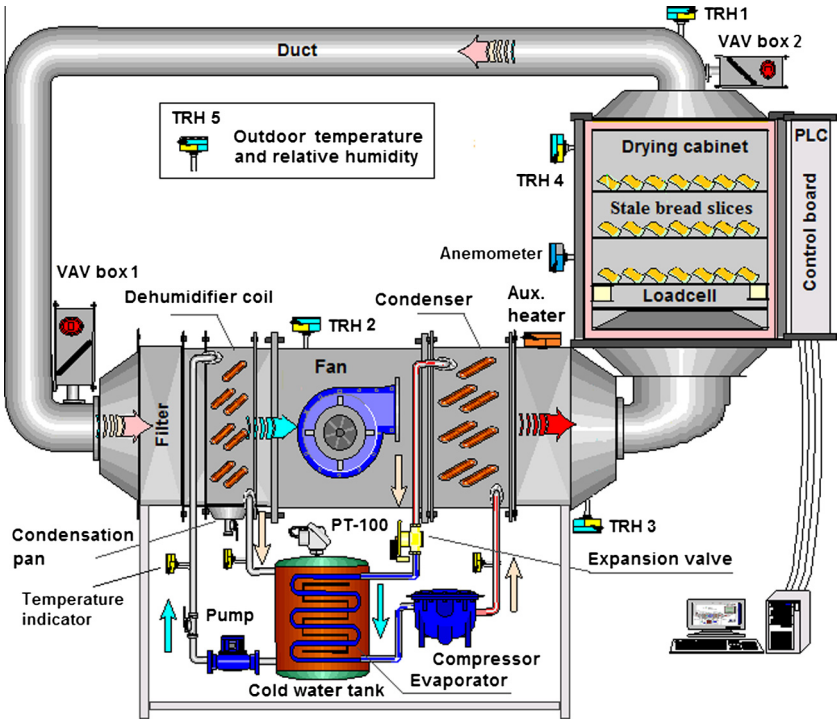

Fig. 2. Closed-loop HPD drying system.

Table 2
Technical characteristics of the equipment used in the HPD system.

Equipments	Technical specifications
Compressor	1/2 hp, R 134a, 220–240 V
Condenser	1 hp
Evaporator	1/2 hp
Fan	100 W, 515 m^3/h, 2750 d/d, 50 Hz, 230 V IN:0.74A
Pump	0.5 hp, 0.37 KW, 220–240 V, 50 Hz, 2.4 m^3/h, H_{max} 40 m, H_{load} 6 m
Cold water tank	40 l
PLC	LCD LED touch screen operator panel 5.7 QVGA, 256-color, 0.9 ms for 1 K scan time, PLC or HMI be used

Table 3
Technical specifications of measurement equipments used in the both dryers.

Devices	Technical properties	Accuracy	Uncertainty
Air flow and temperature measuring device	Velocity 0–20 m/s, temperature −20 to +70 °C, heated wire, NTC sensor	±0.01 m/s ±0.1 °C	±0.0141 m/s ±0.15 °C
Temperature and RH measuring device	5–95% RH, 0 to +70 °C temperature range	±3% ±0.5 °C	±3.42% ±0.7 °C
RH and temperature transmitter	0–100% RH, −40 to +120 °C, operating temperature −10 to + 60 °C	±2% ±1 °C	0.0223% 1.118 °C
Water activity (a_w) measuring device	Value of water activity between 0 and 1	±0.001	±0.002
Digital balance	6100 g max measurement capacity	±0.01 g	±0.0173 g
Thermocouples	Range −200 °C to +850 °C 0–70 °C, supply 24 V-DC, output 4–20 mA	±0.4 °C	±0.648 °C
Weight measuring device	24 VAC 50 Hz or 220 VAC 50 Hz, −40 to +80 °C, 5–12 (DC),	±0.2%,	±0.346%
Load cell	Output (mV/V) 2.0, 5–12 V, 5 kg capacity −40 to +80 °C, 5–12 (DC)	±0.02%	±1.5%
Electric meter	Mono phase, −40 to +70 °C, 3200 Imp/kW h, I_{str} = 20 mA, I_{min} = 250 mA, I_{tr} = 500 mA, I_n = 5a, I_{max} = 80 A	±1%	–
Thermocouple (only HPD)	Pt-100, 6 mm diameter	±0.1 °C	±0.141 °C

2.2. Analysis of systems

Simple theoretical correlations were used to evaluate drying behavior and efficiency of the developed dryers. During drying experiments, the heat delivered by the condensation of refrigerant can be calculated as:

$$\dot{Q}_C = \dot{m}_{ia}(h_{oa} - h_{ia}) \quad (1)$$

The energy balance of dryers;

$$\dot{Q}_{tot} = \dot{Q}_1 + \dot{Q}_2 + \dot{Q}_3 + \dot{Q}_4 + \dot{Q}_5 \quad (2)$$

where $\dot{Q}_1$ is the energy consumption to heat the drying cabinet walls (kW), $\dot{Q}_2$ is the energy needed to heat the drying air (kW), $\dot{Q}_3$ is the energy consumed to heat the dried product (kW), $\dot{Q}_4$ is the energy required for the evaporation of moisture (kW), $\dot{Q}_5$ stand for heat losses to the environment (kW).

Total energy consumption (TEC) of the IRD was divided into three parts. The TEC during infrared drying process was equal to $E_{IRD,1} + E_{IRD,2} + E_{IRD,3}$. Total energy consumption of the IRD (TEC_{IRD}) was expressed with the Eq. (3):

$$TEC_{IRD} = E_{IRD,1} + E_{IRD,2} + E_{IRD,3} \quad (3)$$

where $E_{IRD,1}$ is the energy required for the infrared heaters (kW h), $E_{IRD,2}$ is the energy consumption of fans (kW h), and $E_{IRD,3}$ stands for recovered energy at the HR; and value of $E_{IRD,3}$ depends on the usage of HR.

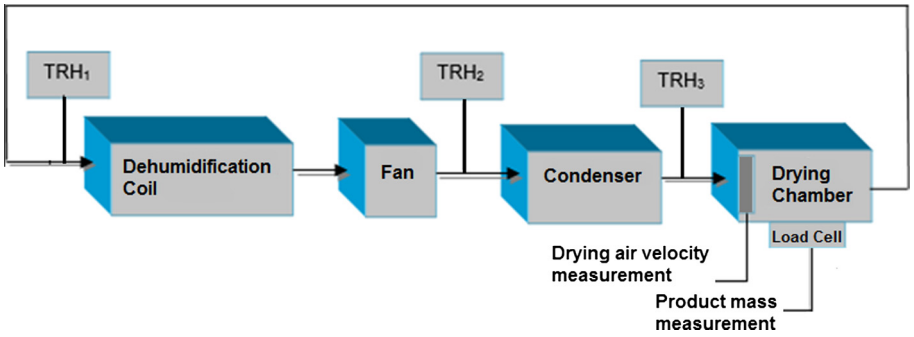

Fig. 3. Air flow and measurement points of the HPD system.

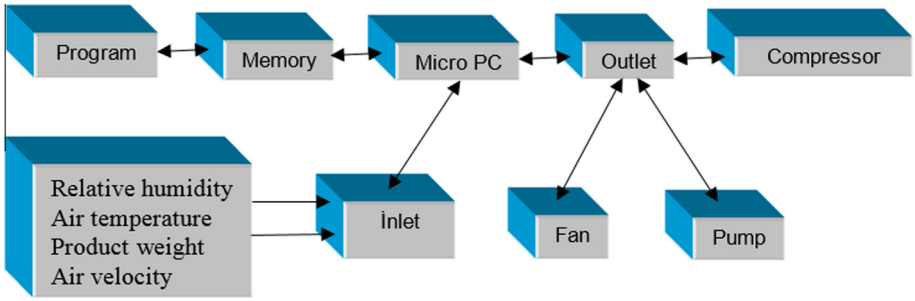

Fig. 4. Control system of the HPD.

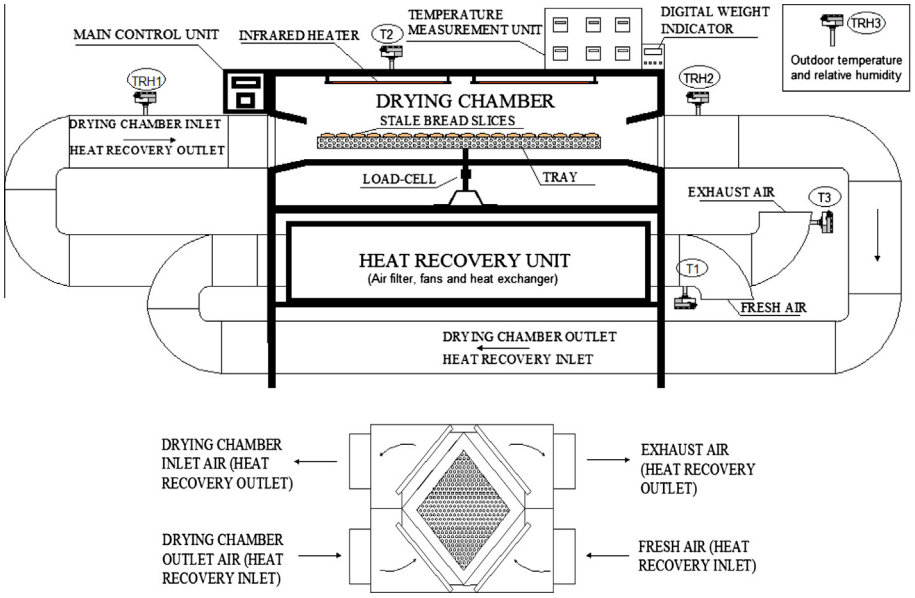

Fig. 5. Infrared drying system and the details of the heat recovery unit.

Eq. (4) gives total energy consumption (TEC_{HPD}) of the HPD as below:

$$TEC_{HPD} = E_{HPD,1} + E_{HPD,2} + E_{HPD,3} \quad (4)$$

where $E_{HPD,1}$ is the energy consumption of compressor (kW h), $E_{HPD,2}$ is the energy consumption of blowing drying air (kW h), and $E_{HPD,3}$ is the energy consumption of water pump of dehumidification unit.

The energy consumption of the fan with regard to the frequency value was estimated during the experiments by means of the following equation. Besides, energy consumption of fans was measured for better results using the instrumentation method. Fan frequency value was fixed at a constant value in both dryers.

$$\left(\frac{n_1}{n_2}\right)^3 = \frac{P_1}{P_2} \quad (5)$$

The coefficients of performance of the heat pump (COP_{HP}) and the coefficient of performance of the whole system ($COP_{ws,HP}$) can be defined as [24]:

$$COP_{HP} = \frac{\dot{Q}_C}{\dot{W}_{Comp}} \quad (6)$$

$$COP_{ws,HP} = \frac{\Sigma \dot{Q}}{\Sigma \dot{W}} = \frac{\dot{Q}_C}{\dot{W}_{Comp} + \dot{W}_F + \dot{W}_P} \quad (7)$$

Table 4
Technical characteristics of the equipments used in the IRD system.

Equipments	Technical specifications
Heat recovery device	230 V 50 Hz, max. flow rate 1000 m^3/h, fan power 265 W
Infrared lamp	Rod type 235 V, 6 × 500 W, 410 mm length
Electricity meter	220 V, 50 Hz, one-phase TS EN 62052-11, −40 to +85 °C, 8 digits LCD display
Control board	220 V AC, 10 A, 0–80 °C range, accuracy ±0.1 °C, intervals of 0.5 Hz frequency control of Rs485–modbus protocol

The mechanical and thermal energy consumed by drying system equipment were calculated using Eqs. (8) and (9) [25].

$$EU_{mec} = \Delta P \cdot \dot{V}_a \cdot t \tag{8}$$

$$EU_{ter} = (A \cdot v \cdot \rho_a \cdot c_{pa} \cdot \Delta T + P \cdot t) \cdot 3600 \tag{9}$$

The energy used for moisture evaporation was calculated using Eq. (10).

$$Q_w = h_{fg} \cdot m_{w,eV} \tag{10}$$

The necessary energy to heat the wet product was calculated using Eq. (11).

$$Q_m = m_p \cdot c_{pp} \cdot (T_{p,o} - T_{p,i}) \tag{11}$$

The specific moisture extraction rate (SMER) can be defined as the energy required for water evaporation. The SMER values were calculated by means of the following equations [26].

$$SMER_{HP} = \frac{\dot{m}_{Water}}{\dot{W}_{Comp}} \tag{12a}$$

$$SMER_{ws,HP} = \frac{\dot{m}_{Water}}{\Sigma \dot{W}} = \frac{\dot{m}_{Water}}{\dot{W}_{Comp} + \dot{W}_F + \dot{W}_P} \tag{12b}$$

$$SMER_{IR} = \frac{\dot{m}_{Water}}{\dot{W}_F + \dot{W}_{IR}} \tag{12c}$$

The energy utilization ratio (EUR) in drying cabinet can be estimated by the following equation:

$$EUR = \frac{\dot{m}_{ia} \cdot (h_{ia} - h_{oa})}{\dot{m}_{ia} \cdot c_p \cdot (T_{ia} - T_{aai})} \tag{13}$$

The energy efficiency of the drying systems can be formulized as below:

$$\eta_{ws,ee} = \frac{Q_w}{EU(ter + mec)} \tag{14}$$

The drying efficiency of the systems can be expressed as below:

$$\eta_{ws,de} = \frac{Q_w + Q_m}{EU(ter + mec)} \tag{15}$$

The moisture content (MC), moisture ratio (MR) and drying rate (DR) of the products during drying experiments can be estimated by means of the following equations:

$$MC_{db} = \frac{M_i - M_d}{M_d} \cdot 100 \tag{16}$$

$$MR = \frac{M - M_e}{M_0 - M_e} \tag{17}$$

$$DR = \frac{M_{t+dt} - M_t}{dt} \tag{18}$$

Reynolds number, Nusselt number and heat transfer coefficient as follows [27]. According to definition of Nusselt number, convection heat transfer coefficient of bread in contact with air flow can be calculated by Eq. (19c) that is necessary for extracting cooling effect in Eq. (19d).

$$Re = \frac{uLs}{\upsilon} \tag{19a}$$

$$Nu = 0.453 Re^{0.5} Pr^{1/3} \tag{19b}$$

$$\hbar = \frac{Nu\ k}{Ls} \tag{19c}$$

$$Q_{air} = \hbar A_s (T_s - T_i) \tag{19d}$$

Convective mass transfer coefficient can be calculated from Biot number (Bi) as follows [27].

$$Bi = \frac{h_m L}{D_e} \tag{20a}$$

The Biot number can be calculated according to Dincer number relationship and Biot number in equation [28].

$$Bi = \frac{24.85}{Di^{0.375}} \tag{20b}$$

$$Di = \frac{u}{k_c L} \tag{20c}$$

where k_c is drying constant that can be defined by the following expressions [29]

$$-k_c(MC - MC_{eq}) = \frac{dMC}{dt} \tag{20d}$$

Total uncertainty values can be estimated through the following equation [30]:

$$W_R = \left[\left(\frac{\partial R}{\partial x_1} w_1 \right)^2 + \left(\frac{\partial R}{\partial x_2} w_2 \right)^2 + \cdots + \left(\frac{\partial R}{\partial x_n} w_n \right)^2 \right]^{1/2} \tag{21}$$

The output of a proportional temperature controller used in the IRD can mathematically be expressed as:

$$P_{out} = K_P e(t) + p0 \tag{22}$$

where P_{out} is output of the proportional controller, p_0 is controller output with zero error, K_p is proportional gain and $e(t)$ is instantaneous process error at time t.

The process path of air in the HPD and the IRD on the Psychrometric chart are shown in Figs. 6 and 7.

2.3. Preparation phase in drying process

In all experiments, loaf of stale bread was sliced the same thickness (sliced into 15 mm, ±0.4 mm) and same properties. Before the experiments, the initial moisture content of the sliced stale bread was determined according to AACC, 2000 [31]. Sliced breads were kept waiting under the natural conditions for going stale. Initial moisture content of the stale bread slices was calculated as 0.55 g water/g dry matter. The average product load was calculated as 3673 g/m^2 for dryers.

2.4. Implementation of experiments

For the efficient experiments, the safe storage period to maintain quality of sliced stale bread and the drying conditions were determined. In order to foresee and avoid mistakes in experiments, they were commenced by reviewing all possible circumstances, including side-effects. Energy consumption and drying behavior were monitored to evaluate the dryers. Specific energy consumption and drying time were evaluated under the same conditions.

Nine experiments were performed at different drying air temperatures (40, 45, 50 °C) and at different air velocities (0.5, 1, 1.5 m/s) in the HPD. The most efficient working conditions of HPD were obtained at 45 °C DAT and 1 m/s DAV. Accordingly, three experiments were conducted at 45 °C drying air temperature and

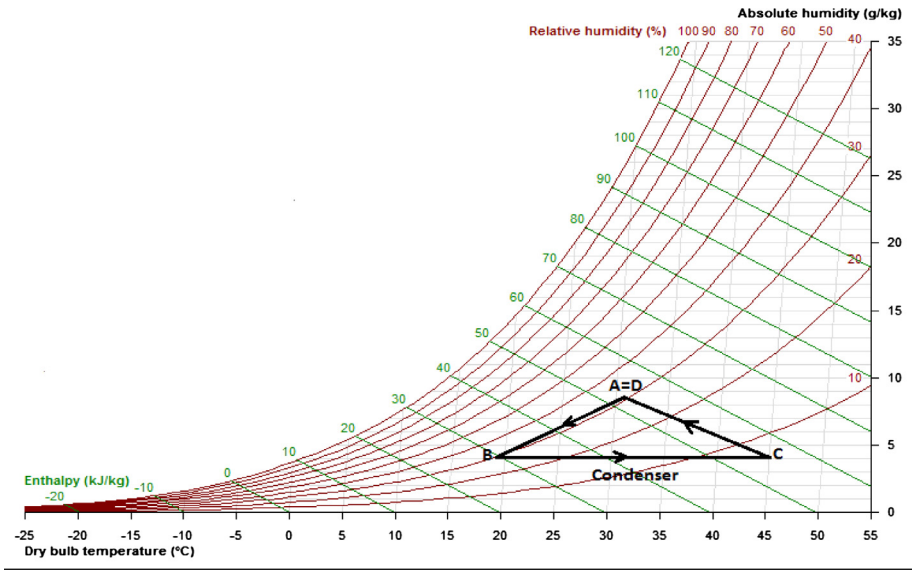

(A=D) - B → Dehumidification of drying air
B - C → Sensible heating with condenser
C – (D=A) → Drying air inlet-outlet to drying cabinet

Fig. 6. The process path of air in HPD on the psychrometric chart.

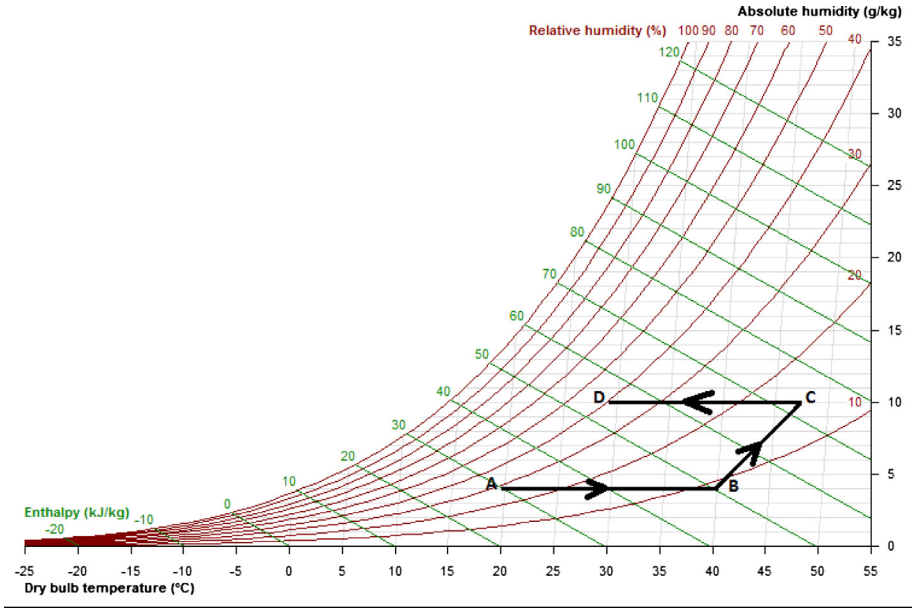

A - B → Sensible heating in heat recovery device
B - C → Drying air inlet-outlet to drying cabinet
C - D → Sensible cooling in heat recovery device

Fig. 7. The process path of air in IRD on the psychrometric chart.

0.5, 1, 1.5 m/s drying air velocities in the IRD to compare and analyze the both systems.

3. Results and discussion

3.1. Performance of the systems

This study focuses on performance analysis of the HPD and the IRD. In addition, it investigates the effects of both systems on the drying characteristics of the stale bread slices. As it is known, during the drying process, enzymatic browning occurs at high temperatures of drying air. There are two ways to reduce browning. The former is implementing drying process under vacuum; the latter is implementing drying process at low drying temperatures. The HPD was tested under different psychometric conditions. Ambient temperature and relative humidity is also influencing the performance of the dryer. The ambient temperature values ranged from 22 to 23 °C while the relative humidity values were ranged between 22% and 24%. The average RH value of drying air across nine experiments was measured as 11.4%; and it was varied

between 3.8% and 22.6% during the HPD test. During the drying process, the drying air did not provide for a fertile environment to microorganisms on sliced breads because its water content was sufficiently low. It was observed that there are two main advantages with the drying processes conducted within low RH conditions. The first one is drying time shortened compare to system that conducted under conditions without RH control, and the second one is moisture extraction rate of drying air increased in compare to the conventional system.

According to the experimental results, the highest $COP_{ws,HP}$ was obtained as 3.7 at 45 °C DAT and 1 m/s DAV (Table 5). As it can be seen in Table 4, as DAT was increased above 45 °C, the COP_{ws} value was decreased for the HPD.

Removing moisture from product was significantly influenced by air temperature and its flow rate (Table 6). Increasing DAV in the IRD process resulted in several effects such as reduction in mass transfer, increase in energy consumption, extension in drying time and increase heat loss from drying cabinet wall and cooling effect of dried stale bread. We concluded that 0.5 m/s drying air velocity is the optimum value in the infrared drying of monolayer bread slices with respect to drying efficiency and time. The higher the DAV (above 0.5 m/s) caused longer drying time in the IRD. When the DAV is increased during the infrared drying, the drying rate is significantly decreased. The specific energy consumption is decreased by reducing the air flow rate in IRD system. Additionally, it was observed that increasing in radiation rate affects moisture removal rate directly also, the gained radiation energy is a function of distance between the lamps and the bread slices. In the IRD system, the experiments were conducted for different bread surface-lamp distances (100 mm, 200 mm and 300 mm). When the distance between the lamps and the product was 100 mm, it caused regional browning on the dried bread surface. It is observed that the flux of water increased, as the distance between the lamps and the bread decreased. On the other hand, increasing in distance will decrease the water flux. Moreover, the energy consumption increased due to the longer distance (300 mm). Optimum distance between the lamps and the bread surface was determined as 200 mm. Similar results were reported by Nowak and Lewicki [2]. It can be concluded that air flow above the bread surface has two effects: conveying evaporated water from bread surface and cooling effect. It should mention that high flow velocity increases the cooling effect while the evaporation rate decreases by falling down the surface temperature. Therefore the optimum air velocity is needed to make a balance between bread cooling and removal evaporated moisture. High air velocity has significant effect on drying kinetics of bread and energy consumption as observable in Table 6. The air flow velocity variation has stronger role on cooling effect and evaporation rate in compare with temperature variation.

It was found from the results of the experimental investigation that the drying air temperature, drying air velocity, dried product properties and drying air relative humidity have important roles for the total drying time and drying efficiency. Based on the experiment results of the IRD system, appropriate drying conditions to obtain the highest drying efficiency and drying rate were measured at 0.5 m/s DAV. As the DAV and DAT are increased, energy consumption is also increased. As it is known, when the product is exposed to long-term high temperatures through infrared heating, it causes discoloration and regional browning on the bread surface. However, drying at low temperatures requires longer drying process time, and thus it causes higher energy consumption. As a result, the bread slices can be dried at the highest possible quality, if they are not exposed long-term direct-infrared-radiation. Similarly, this phenomenon is explained by Krishnamurthy et al. [32]. The results of the present study showed that the PC of power has positive effect on the energy consumption and drying time.

The IRD and the HPD systems were compared at the same optimum conditions at 45 °C DAT and 1 m/s DAV. Energy consumption of dryers was evaluated by using experimental data. Energy consumptions of the IRD and the HPD systems during the experiments (45 °C DAT-1 m/s DAV) are shown in Fig. 8. As it can be seen in Tables 5 and 6, drying periods of experiments conducted at 45 °C – 1 m/s in the HPD and the IRD systems were 45 and 145 min; and their relevant total energy consumptions were 1.089 and 0.760 kW h, respectively. In the IRD system, there was a HR system utilized to heat fresh air. As it can be seen in Fig. 8 dried bread can be quickly affected by infrared lamps while they were heated to reach the set temperature. On the other hand, reaching the desired DAT (45 °C) level needs long time for the HPD system. The amount of energy (kW h) gained from exhausted air in the drying system at 45 °C DAT and 1 m/s DAV was shown in Fig. 8. Total energy consumption of the IRD system was measured as 0.76 kW h, while the gained energy with HR was measured as 0.421 kW h.

Generally IRD systems consume high amount of energy, except the ones with heat recovery capability. Designed IRD system has 35.6% energy saving capability, due to the fact that IRD system has a HR unit. In IRD system without HR unit, the total energy consumption of this IRD system would exceeds the total energy consumption of HPD system (1.181 kW h in IRD_{ec} without HR unit >1.089 kW h in HPD_{ec}).

Cooling capacity in cooling serpentine, cold water temperature value and the amount of heat delivered by the condenser (1 hp) in the HPD system were shown in Fig. 9. The fluctuation of the energy delivered by the condenser was derived by means of simultaneous control of drying air temperature and the RH. The exhaust drying air constitutes a heat source for the evaporator (1/2 hp) due to utilization of a closed-loop system. Therefore, the thermal balance of heat pump and the relative humidity control of drying air were provided efficiently through utilization of cold water. Similarly, heat recovery device was used for sensible heating of drying air in the IRD system. The compressor was controlled on/off loop according to temperature of the influxing drying air into the drying cabinet. Energy mobility in HPD is shown in Fig. 9. As it is shown in Fig. 9, temperature fluctuation was greater than the proportional control.

The SMER values were calculated using Eqs. (12a)–(12c). The $COP_{ws,HP}$ value for the HPD system was calculated using Eq. (7).

Table 5
Experimental results in the HPD system.

Air conditions (°C m/s)	Drying time (min)	$COP_{ws,HP}$	Energy consumption (kW h)
40–0.5	235	2.75	1.505
40–1	205	3.19	1.325
40–1.5	180	3.48	1.242
45–0.5	175	3.05	1.405
45–1*	145*	3.7*	1.089*
45–1.5	130	3.6	1.195
50–0.5	140	2.8	1.415
50–1	115	3.22	1.276
50–1.5	95	3.16	1.31

* Experiment compared with IRD.

Table 6
Experimental results in the IRD system.

Air conditions (°C m/s)	Drying time (min)	Energy consumption (kW h)
45–0.5[a]	38[a]	0.6[a]
45–1[b]	45[b]	0.76[b]
45–1.5	65	1.35

[a] The best result according to 3 experiments.
[b] Experiment compared with HPD.

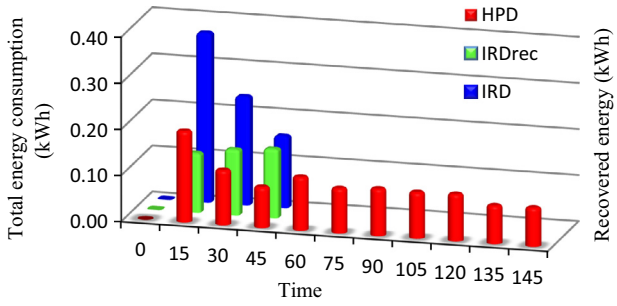

Fig. 8. Total energy consumption and recovery in dryers (45 °C – 1 m/s).

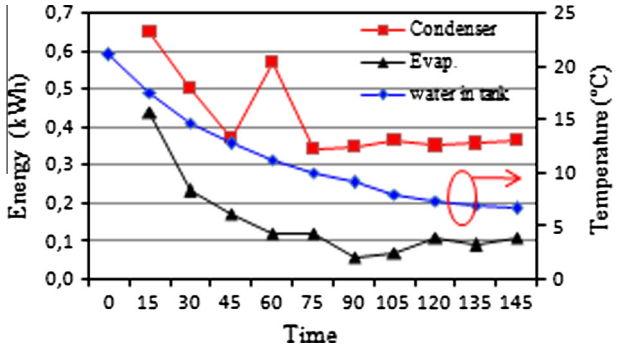

Fig. 9. Energy mobility in HP unit.

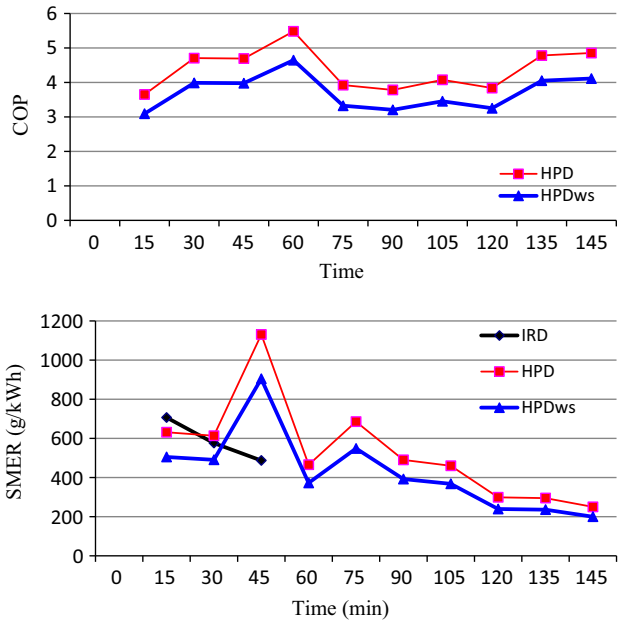

Fig. 10. The COP and the SMER values of the IRD and the HPD systems during the experiments (45 °C – 1 m/s).

Instantaneous max value of the $COP_{ws,HP}$ was obtained 4.3, while average value was calculated as 3.7. Varying COP and SMER values of the HPD system at 45 °C DAT and 1.0 m/s DAV are demonstrated in Fig. 10. Thermodynamic balance of the closed-loop HPD system exhibited stable performance in terms of high $COP_{ws,HP}$, controllable RH of drying air and operation without an auxiliary heater. The SMER values of the IRD and the HPD systems were 487.1–706.5 g/kW h and 250–1130.6 g/kW h, respectively. The average SMER values of the IRD and the HPD systems were 590 g/kW h and 425 g/kW h, respectively. It was concluded that the IRD system was more energy-efficient compared to the HPD system. It was determined that the initial moisture content of bread slices, mobility of product and bread weight have effect on the SMER value. During the drying tests, the EUR values were calculated within the range of 17% and 65% by the Eq. (13). The energy consumption shares of dryers are shown in Fig. 11. In the mean time, the figure exhibits the energy saving points and the potential to reach the highest energy efficiency.

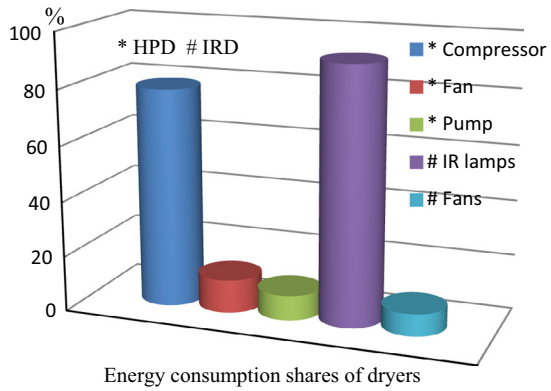

Fig. 11. Energy consumption shares of dryers (45 °C – 1 m/s).

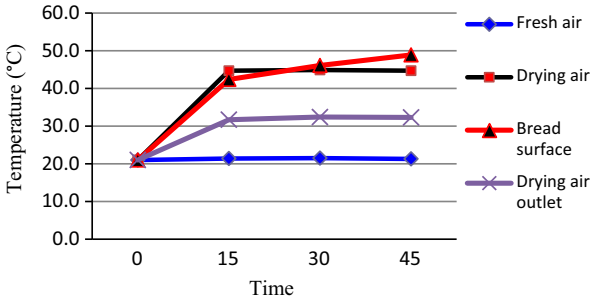

Fig. 12. Temperature variations in the IRD system (45 °C – 1 m/s).

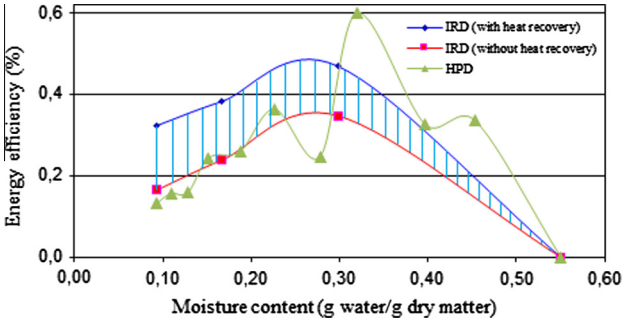

Fig. 13. The overall energy efficiency of dryers (45 °C – 1 m/s).

Temperature variations in the IRD system are shown in Fig. 12. At the end of the infrared drying process, surface temperature of stale bread slices exceeded the temperature of drying air. During the absorption of the infrared rays by the product, evaporation prevents product surface temperature increasing at beginning drying stages. As the amount of moisture decreased in the product, its surface temperature increased. Whereas the product surface temperature reached about 40 °C in the HPD system, it reached about 49 °C in the IRD system. Consequently, PC prevented overheating

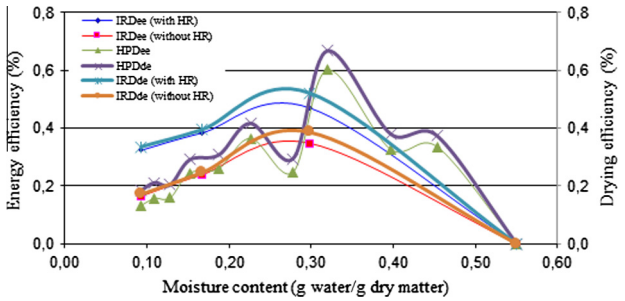

Fig. 14. Variations in energy and drying efficiencies of dryers (45 °C – 1 m/s).

of the product in the IRD system. Non-uniform drying and product overheating occurs if IRD system is used without PC.

The system efficiencies of both dryer were estimated using Eqs. (14) and (15). Energy efficiency variations were shown in Figs. 13 and 14. In Fig. 13, the scanned area between the IRD with HR and IRD without HR shows energy saving potential of HR. The energy efficiency of IRD with HR, the IRD without HR and the HPD system were calculated within the ranges of 32–47% (average 39%), 17–35% (average 25%) and 13–60% (average 28%), respectively. As it can be seen in Fig. 13, the reasons of fluctuation of drying efficiency values in HPD are due to convective drying and simultaneous RH and temperature control of drying air in closed-loop cycle. So, the maximum energy efficiency value was obtained as 60% in the HPD system. The drying efficiency of IRD with HR, the IRD without HR and the HPD system were calculated within the ranges of 34–52%, 17–39% and 19–67%, respectively. These efficiency values can be increased with the usage of energy-efficient devices such as compressor with frequency converter, more efficient electrical devices and insulation materials.

3.2. Analysis of drying characteristics

The stale bread was sliced to aid quick drying and placed on wire grid within the drying cabinet as shown in Fig 15. In the dryers similar conditions taking into account many factors were created. The effects of drying conditions on the drying behavior of stale bread in both dryers were determined. Drying characteristic is a very important factor that clearly determines the performance of dryer. Therefore, recently, there have been many studies on the drying characteristic [33–35]. The drying curves were obtained by calculating the MC, MR and DR values as a time function under particular drying air conditions. These variations during the experiments were calculated with Eqs. (16)–(18) and variations in MC, MR, DR, DR-MC and MR-MC are exhibited in Fig. 16. In drying systems, moisture content of bread slices was gradually decreased from 0.55 g water/g dry matter to 0.09 g water/g dry matter. As it can be seen in Fig. 16, the drying rate of the IRD system was higher than the HPD system. In the IRD system, measured radiation intensity was in the range of 0.1875–0.9375 W/cm^2. The MC and the DR values were affected by increasing radiation intensity. It can be concluded that drying time can be reduced by increasing density of infrared power.

Water flux values of the IRD and the HPD systems were calculated as 0.54 g/m^2 s and 0.16 g/m^2 s, respectively. It was observed that the disadvantage of convective drying was taking longer time and consumes more energy to maintain thermal balance between the temperatures of product surface and the drying air. It was also observed that the important advantage of the infrared drying process was shorter heating period required for product to reach the desired conditions. According to the experimental results (45 °C – 1 m/s), at the fifteenth minute, temperature measurement values for drying air and surface of the drying bread slices were nearly equal to each other in the infrared drying process.

At the first 15-min period of experiments, DR_{IRD} was 2.83 times higher than DR_{HPD}. At the fifteenth minute of experiments, while the MC_{IRD} was about 0.30 g water/g dry matter, the MC_{HPD} reached this value at the forty-fifth minute. At the fifteenth minute of experiments, while the MR_{IRD} was about 0.54, the MR_{HPD} was about 0.82 at the forty-fifth minute. At the end of experiments, the average drying rate of the IRD system was found 3.3 times higher than the drying rate of the HPD system. Qualitative drying process is desirable by shortening the time. Each dryer describes the drying behavior of sliced stale bread.

This dryer processes can be classified in both internally and externally controlled period for this study, due to Bi_m number were obtained in the range of $0 < Bi_m < 100$. Variation of effect moisture diffusivity (D_e) and mass transfer coefficient (h_m) is shown in Fig. 16. These values of a food are internal factors related to properties of food. The D_e values are reported within the general ranges of 10^{-9}–10^{-11} m^2/s for food and agricultural materials [33]. But it was observed the effect moisture diffusivity (D_e) during drying of stale bread slices, where this coefficient varied from 8.3×10^{-8} to 3.2×10^{-7} m^2/s. Nevertheless, due to harmony of temperature and air velocity used, and porous structure of the bread in this work, the values of D_e were larger than it reported for others materials (Fig. 17). Maroulis et al. were stated that the self-diffusivity of water is approximately 10^{-8} m^2/s, and the D_e value in bone-dry food material can be lower [36]. Also, low D_e values are found in non-porous and sugar-containing foods, however higher values of D_e characterize porous food materials. In addition, D_e values varied from 2.86 to 5.4×10^{-8} m^2/s with the blanched samples having higher values by Tunde-Akintunde [37]. In this study of bread has been observed the effect of temperature on D_e. D_e values showed dependency on infrared power and condenser capacity.

Fig. 15. View of product within drying cabinets.

The average values of the h_m were 4.52×10^{-5} m/s in IRD and 1.17×10^{-5} m/s in HPD.

Water activity (a_w) and water binding capacity (WBC) and color of product are determinant parameters for the quality of the dried product. a_w is an important quality indicator of dried foods. It is an important characteristic of ultimate products; and it can be described as below:

$$a_w = p/p_0 \tag{23}$$

where p is the vapor pressure of water in the substance, and p_0 is the vapor pressure of pure water at the same temperature.

Mold growth that causes spoilage of the bread limits shelf life of bread. The growth of most harmful microorganisms can be limited by reducing water activity below 0.60 or moisture content below 10% [38]. While water activity levels of fresh bread are in the range of 0.9–0.95; a_w of bread crumbs must be in the range of 0.65–0.66 [39]. The a_w measurement device determined the a_w as 0.335 and 0.348 (at 25 °C ambient temperatures) for the IRD and the HPD systems, respectively. Accordingly, a_w values obtained were ideal to storage safely.

WBC (g water/g db) was used as indicator of the quality of the dried bread samples. WBC of the sample was measured according to the procedure described by Medcalf and Gilles [40] and measurements were performed in triplicate.

$$\text{WBC} = \frac{\text{Weight of treated sample} - \text{Initial weight of sample}}{\text{Initial weight of sample}} \tag{24}$$

The WBC values were obtained as 1.92–2.47. In conventional dryer WBC value is low however it is high in infrared dryer. WBC values can be affected by many factors such as content or temperature. During drying, WBC values of the bread crumbs are related to the extent of the influence of the drying time and infrared heating rate. Infrared drying method was effective on the WBC value of bread slices as compared to conventionally dried bread slices. Another quality indicator is color. There was a noticeable increase in color saturation of the product with temperature increase. Color of dried bread slices with hot air was lighter than infrared-dried bread slices. The best result based on WBC was achieved when samples were dried with IRD. However, the best result based on minimum color change achieved when samples were dried with HPD.

Artificial Neural Network (ANN) applications cope with problems by the login information. The ANN model was used to predict the energy consumption (EC) of the HPD and IRD system. EC depends on drying air temperature, drying air velocity and drying time. The network inputs are drying air temperature (T), drying air velocity (v) and drying time (t), whereas the output of network is EC. The FERMI transfer function is given by the following equation.

The transfer function is:

$$F_{(z)} = \frac{1}{1 + e^{-4(z-0.5)}} \tag{25}$$

where z is the weighted sum of the input.

ANN has been modeled by "Pythia" computer software. We have used 4 neurons, 2 levels, 3 inputs and 1 output. For the prediction EC of HPD and EC of IRD have been obtained from following equations;

$$F_{(EC-HPD)} = \frac{1}{1 + e^{-4(-2.425740631612\,T - 0.645692091533\,v - 0.744732095028\,t - 0.5)}} \tag{26}$$

$$F_{(EC-IRD)} = \frac{1}{1 + e^{-4(-1.6234471811\,T + 0.119713768013\,v + 7.722117058355\,t - 0.5)}} \tag{27}$$

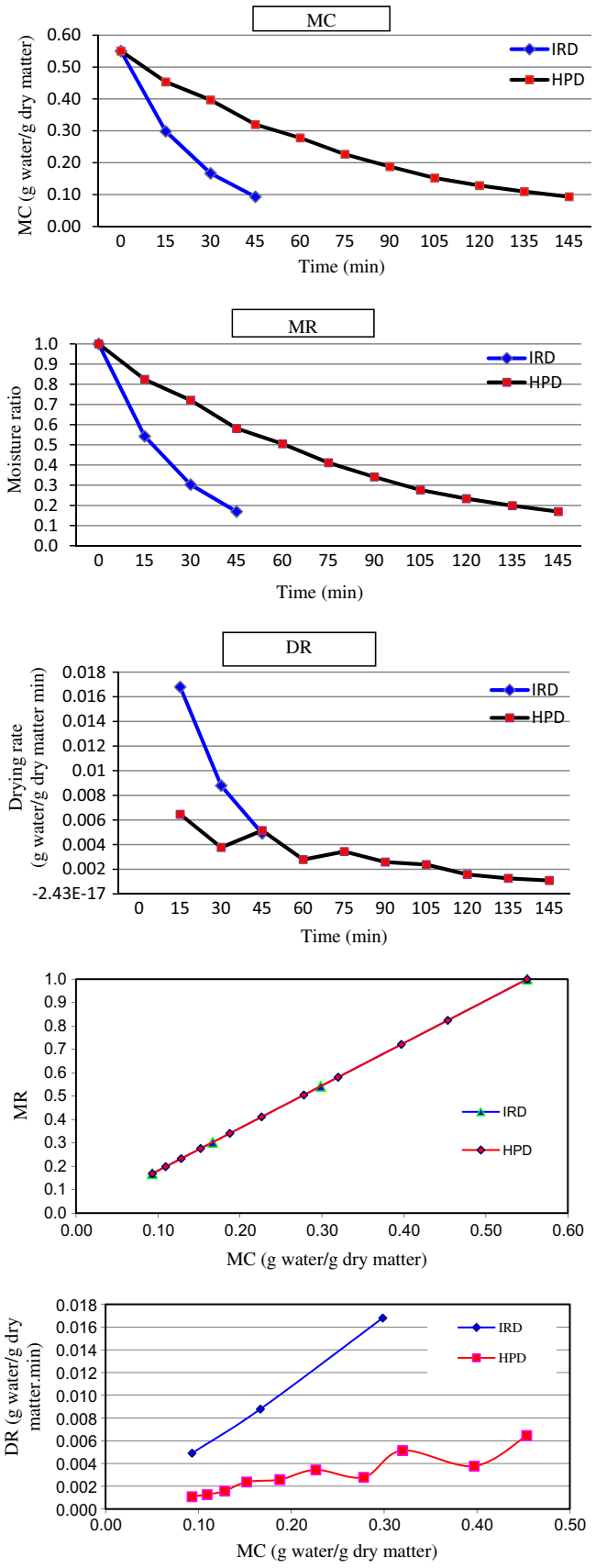

Fig. 16. Drying kinetics of sliced bread (45 °C – 1 m/s).

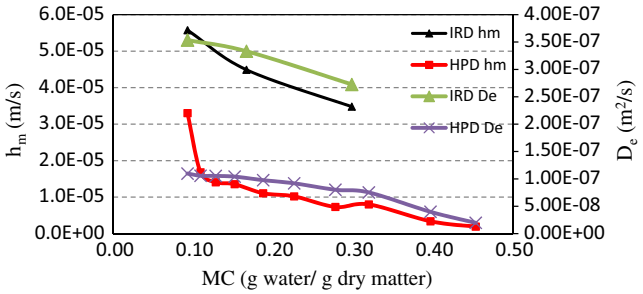

Fig. 17. Mass transfer on sliced bread (45 °C – 1 m/s).

Table 7
N_{min} and N_{max} values.

	Input 1 (T)	Input 2 (v)	Input 3 (t)	Output
HPD system				
max	50	1.5	235	1.505
min	40	0.5	95	1.089
RD system				
max	46	1.5	65	1.35
min	45	0.5	38	0.6

Input and output layers are normalized in the (0, 1) range. Where, N_{act} is the actual value, N_{min} and N_{max} are minimum and maximum values in the data set, respectively [12].

$$N_N = \frac{N_{act} - N_{min}}{N_{max} - N_{min}} \quad (28)$$

Firstly, input values are normalized in the (0, 1) range with usage of Eq. (28). Then, output values will be normalized by using N_N value to obtain the N_{act} value. For normalization application, the N_{min} and N_{max} values are given in Table 7.

R^2 and average error values of EC of HPD and EC of IRD were determined as 1 and 0.9999, 0.0005% and 0.0098%, respectively. Thus it is seen that the model is suitable.

Some previous studies are given in Table 8 to compare important drying system parameters between the obtained values and the literature. The heat transfer mechanism, product properties, mobility product, new technologies and energy saving applications affect the energy efficiency of dryers. In this regard, as it can be seen in Table 8, experimental values which are obtained from this study are effective and sustainable when comparing with the literature.

4. Conclusions

In this study, the HPD and the IRD systems were developed and tested at low drying air temperatures. Efficient approaches have been introduced to the industrial drying applications such as usage of HR, PC of drying air temperature for the IRD and accurate RH control with closed-loop system for the HPD. Due to DAV, DAT and RH are important factors in the drying process; their values were optimized to obtain the maximum performance and drying efficiency. The advantages of these food dryers are presented below:

- The food is not exposed to long term infrared radiation due to PC of temperature. So, uniform heating and drying have been obtained in IRD.
- In the IRD system, HR provided 35.6% energy saving.
- The IRD system with HR provided the highest average whole system efficiency. The HR device contributed by 14% on whole system energy efficiency. The whole system energy efficiency of the HPD system was calculated within the range of 13–60% (average 28%).

Table 8
Design and performance evaluation of dryers.

Refs.	Drying system	DAT (°C)–DAV (m/s)	Drying time (min)	Material	Drying efficiency (%)	SEC (kJ/kg)	Infrared power	COP_{WS}
[41]	HA	80–1	345	Patato	–	17,170	–	
	HA		345	Carrot	–	16,150	–	
	IRD		285	Patato	–	7600	–	
	IRD		285	Carrot	–	7150	–	
	HAIRD		180	Patato	–	6430	–	
	HAIRD		180	Carrot	–	6040	–	
[42]	IRD	35 °C	510	Onion slices	–	–	300 W	
		40 °C	480		–		300 W	
		45 °C	468		–		300 W	
		35 °C	420		–		400 W	
		40 °C	420		–		400 W	
		45 °C	360		–		400 W	
		35 °C	330		–		500 W	
		40 °C	270		–		500 W	
		45 °C	240		–		500 W	
[43]	IRD	60–2	220	Onion slices (2 mm)	–	–	–	–
		70–2	160					
		80–2	140					
		60–1.4	260					
		60–0.8	320					
[44]	HPD	55–2.7	420	Hibiscus, mint, parsley	–	4029	–	–
		55–2.7				3982		
		55–2.7				3684		
[25]	IRD	0.5 m/s	110	Daisy	13.97	40,000	0.49 W/cm²	
		1 m/s	170		7.55		0.31 W/cm²	
		1.5 m/s	285		3.7	140,000	0.22 W/cm²	
This study	HPD	45–1	145	Bread slices	33	–	–	3.7
	IRD	45–0.5	38		–		–	
		45–1	45		27	–	0.1875–0.9375 W/cm²	
		45–1.5	65		–		–	

- Drying air flow rate was kept ±1.16% accuracy with the PID control in the HPD system.
- Drying air RH was controlled accurately in the range of 3.8–22.6% for the HPD system.
- In the experiments, the optimum drying air velocity was obtained as 0.5 m/s for the IRD system and whereas it was obtained as 1 m/s for the HPD system. Increasing air velocity in the IRD system decreases the energy efficiency in the whole system while it shortens drying time in the HPD system.
- The highest average $COP_{ws,HP}$ value was calculated as 3.7 at 45 °C DAT and 1 m/s DAV by controlling the both DAT and RH.
- When the both systems were compared in terms of the drying time, the IRD system shortened required time up to 69% and also it reduced the energy consumption by 43.2%.
- D_e value during drying of stale bread slices varied from 8.3×10^{-8} to 3.2×10^{-7} m^2/s. Average values of the h_m were found as 4.52×10^{-5} m/s and 1.17×10^{-5} m/s for dryers.
- It can be concluded that both systems are effective methods for removal of water content. Both dryer systems can be used in production process of bread crumb in the food industry. Thus, it can contribute to reduction in wastage of bread in society.

The infrared drying process is faster than heat pump drying based on the equivalent parameters. A system composed of a combination of both dryers can be more efficient. Infrared-assisted closed type heat pump system can bring energy and time saving, due to technical properties of both system, such as infrared drying system's superior capability for removal of surface moisture, and the HPD system's superiority in control of relative humidity together. Additionally, solar energy or other alternative energy sources can be utilized successfully in the both dryer systems. Applied techniques which are increased the drying efficiency can be used for industrial drying systems.

References

[1] Şevik S. Experimental investigation of a new design solar-heat pump dryer under the different climatic conditions and drying behaviour of selected products. Sol Energy 2014;105:190–205.
[2] Nowak D, Lewicki PP. Infrared drying of apple slices. Innovative Food Sci Emerging Technol 2004;5:353–60.
[3] Sui Y, Yang J, Ye Q, Li H, Wang H. Infrared, convective, and sequential infrared and convective drying of wine grape pomace. Dry Technol 2014;32(6):686–94.
[4] Jaturonglumlert S, Kiatsiriroat T. Heat and mass transfer in combined convective and far-infrared drying of fruit leather. J Food Eng 2010;100:254–60.
[5] Minea V. Heat-pump–assisted drying: recent technological advances and R&D needs. Dry Technol 2013;31(10):1177–89.
[6] Colak N, Hepbasli A. A review of heat pump drying: Part 1 – Systems, models and studies. Energy Convers Manage 2009;50(9):2180–6.
[7] Prasertsan S, Saen-saby P. Heat pump driers: research and development needs and opportunities. Drying Technol 1998;16(1–2):251–70.
[8] Mohanraj M, Chandrasekar P, Sreenarayanan VV. Performance of a heat pump drier for copra drying. Proc Instit Mech Eng, Part A, J Power Energy 2008;222 (Tech Note 1).
[9] Hammouda I, Mihoubi D. Comparative numerical study of kaolin clay with three drying methods: Convective, convective–microwave and convective infrared modes. Energy Convers Manage 2014;87:832–9.
[10] Rahman SMA, Saidur R, Hawlader MNA. An economic optimization of evaporator and air collector area in a solar assisted heat pump drying system. Energy Convers Manage 2013;76:377–84.
[11] Ceylan İ, Aktaş M. Hazelnut drying in a dryer assisted heat pump. J Fac Eng Arch Gazi Univ 2008;23(1):215–22.
[12] Aktaş M, Şevik S, Özdemir MB, Gönen E. Performance analysis and modeling of a closed-loop heat pump dryer for bay leaves using artificial neural network. Appl Therm Eng 2015;87:714–23.
[13] Zielinska M, Zapotoczny P, Alves-Filho O, Eikevik TM, Blaszczak W. A multi-stage combined heat pump and microwave vacuum drying of green peas. J Food Eng 2013;115:347–56.
[14] Gungor A, Tsatsaronis G, Gunerhan H, Hepbasli A. Advanced exergoeconomic analysis of a gas engine heat pump (GEHP) for food drying processes. Energy Convers Manage 2015;91:132–9.
[15] Nasıroğlu S, Kocabıyık H. Thin-layer infrared radiation drying of red pepper slices. J Food Process Eng 2009;32:1–16.
[16] Motevali A, Minaei S, Khoshtaghaza MH, Amirnejat H. Comparison of energy consumption and specific energy requirements of different methods for drying mushroom slices. Energy 2011;36(11):6433–41.
[17] Aghbashlo M. Exergetic simulation of a combined infrared-convective drying process. Heat Mass Transf 2015. http://dx.doi.org/10.1007/s00231-015-1594-3.
[18] Deng Y, Wu J, Su S, Liu Z, Ren L, Zhang Y. Effect of far-infrared assisted heat pump drying on water status and moisture sorption isotherm of squid (Illex illecebrosus) fillets. Dry Technol 2011;29(13):580–6.
[19] Tireki S, Şumnu G, Esin A. Production of bread crumbs by infrared-assisted microwave drying. Eur Food Res Technol 2006;222:8–14.
[20] Kalkışım, Ö, Özdemir M, Bayram O. Ekmek Yapım Teknolojisi, Gümüşhane University, Gümüşhane Vocational School, 2012. <http://kutuphane.ghu.edu.tr/media/uploads/kutuphane/files/ekmek_yapim_book.pdf>.
[21] TMO, Research a waste of bread in Turkey, Soil Products Office, 2, 10–99, 2013.
[22] John T, Lailach S, Nebelung M, Tscheuschner HD. Fluidized bed drying of bread and biscuit crumbs. J Food Eng 1990;12(1):29–43.
[23] Basman A, Yalcin S. Quick-boiling noodle production by using infrared drying. J Food Eng 2011;106(3):245–52.
[24] Şevik S, Aktaş M, Özdemir MB, Doğan H. Modeling of drying behaviors of mushroom in a solar assisted heat pump dryer by using artificial neural network. J Agric Sci 2014;20:187–202.
[25] Motevali A, Minaei S, Banakar A, Ghobadian B, Khoshtaghaza MH. Comparison of energy parameters in various dryers. Energy Convers Manage 2014;87:711–25.
[26] Aktaş M, Gönen E. Bay leaves drying in a humidity controlled heat pump dryer. J Fac Eng Arch Gazi Univ 2014;29(2):433–41.
[27] Çengel YA, Ghajar AJ. Heat and mass transfer fundamentals and applications. 4th ed. McGraw-Hill; 2011. p. 717–84. Mass Transfer.
[28] Dincer I, Hussain MM. Development of a new Bi-Di correlation for solids drying. Heat Mass Trans 2002;45:3065–9.
[29] Aboltins A. Theoretical study of material drying coefficient. In: 12th conference: Engineering for Rural Development, Jelgava, Latvia, p. 153–8, 2013.
[30] Aktaş M, Şevik S, Doğan H, Öztürk M. Drying of tomato in a photovoltaic and thermal solar-powered continuous dryer. J Agric Sci 2012;18:287–98.
[31] AACC (American Association of Cereal Chemists), Approved Methods of the AACC, 10th ed. AACC, St Paul, MN, USA, 2000.
[32] Krishnamurthy K, Khurana SJ, Irudayaraj J, Demirci A. Infrared heating in food processing: an over-view. Compr Rev Food Sci Food Safety 2008;7:2–13.
[33] Yaoxuan Z, Houhe C, Teng C. Drying kinetics of RDX under atmospheric pressure and vacuum conditions. Energy Convers Manage 2014;80:266–75.
[34] Sarimeseli A. Microwave drying characteristics of coriander (Coriandrum sativum L.) leaves. Energy Convers Manage 2011;52:1449–53.
[35] Taghian Dinani S, Hamdami N, Shahedi M, Havet M. Mathematical modeling of hot air/electrohydrodynamic (EHD) drying kinetics of mushroom slices. Energy Convers Manage 2014;86:70–80.
[36] Maroulis ZB, Saravacos GD, Panagiotou NM, Krokida MK. Moisture diffusivity data compilation for foodstuffs: effect of material moisture content and temperature. Int J Food Prop 2001;4(2):225–37.
[37] Tunde-Akintunde TY. Effect of pretreatments on drying characteristics and energy requirements of plantain (Musa|AAB). J Food Process Preserv 2014;38 (4):1849–59.
[38] Jangam SV, Law CL, Mujumdar AS. Drying of foods, vegetables and fruits, vol. 1, Singapore, 2010.
[39] Cauvain S, Young LB. Food manufacture and quality: water control and effects. 2nd ed. Oxford, England: Wiley & Blackwell; 2008.
[40] Medcalf DG, Gilles KA. Wheat starches. I. Comparison of physicochemical properties. Cereal Chem 1965;42:558–68.
[41] Umesh Hebbar H, Vishwanathan KH, Ramesh MN. Development of combined infrared and hot air dryer for vegetables. J Food Eng 2004;65(4):557–63.
[42] Sharma GP, Verma RC, Pathare P. Mathematical modeling of infrared radiation thin layer drying of onion slices. J Food Eng 2005;71(3):282–6.
[43] Praveen Kumar DC, Umesh Hebbar H, Ramesh MN. Suitability of thin layer models for infrared–hot air-drying of onion slices. LWT–Food Sci Technol 2006;39:700–5.
[44] Fatouh M, Metwally MN, Helali AB, Shedid MH. Herbs drying using a heat pump dryer. Energy Convers Manage 2006;47(15–16):2629–43.